Effects of Symbol Transition Density on Tracking and Acquisition Performance of the Data Transition Tracking Loop at Low Signal-to-Noise Ratios

S. Million and S. M. Hinedi
Communications Systems and Research Section

Effects of the data transition variation on the performance of the digital data transition tracking loop (DTTL) symbol synchronizer are addressed for symbol signal-to-noise ratios and window sizes of interest. The data transition variation will affect the DTTL performance by introducing an additional timing jitter that results in additional receiver loss. Numerical and simulation results for both tracking and acquisition are presented.

I. Introduction

The symbol synchronizer is the heart of a digital communications system as it provides symbol timing to many essential components of a receiver. Examples of subsystems that require proper symbol timing for accurate operation include the matched filter, the signal-to-noise ratio (SNR) estimator, the Costas in-phase and quadrature sum-and-dump filters, as well as various baseband lock detectors. In power-limited channels, the symbol synchronizer usually extracts the symbol timing directly from the noisy signal [1] and is appropriately termed data-derived symbol synchronization. Although this method requires no additional power solely for symbol synchronization, the advantage comes at the cost of requiring adequate transition (zero crossings) in the data symbol sequence. In applications such as space-to-Earth links, the data transition variation is sometimes very low, and typically additional measures are included in the communications system to guarantee adequate symbol synchronization performance. An example might include randomizing the data stream or using Manchester pulse to guarantee transitions. In applications such as Earth-to-space links, however, the data stream is not coded to ensure adequate transitions; this is done mainly to simplify the spacecraft complexity. This article serves to evaluate the tracking and acquisition performance of a commonly used data-derived symbol synchronizer, the digital data transition tracking loop (DTTL), under the environment of data transition variation.

The DTTL symbol synchronizer is used in various receivers, such as the advanced receiver used by the Deep Space Network [2] and the Tracking and Data Relay Satellite System (TDRSS) satellite receivers [3]. Its functional block diagram is shown in Fig. 1, and its operation is described below. The baseband input signal is first passed through two parallel channels: the in-phase channel (on top) monitors the polarity of the actual transitions, and the quadrature channel (on the bottom) measures the timing error.

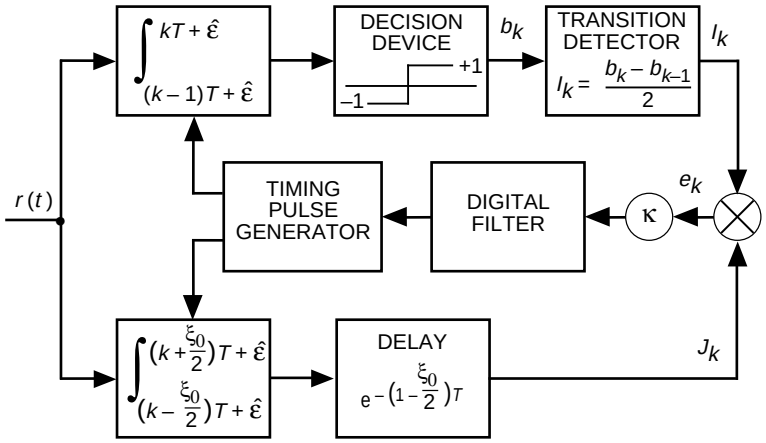

Fig. 1. The digital data transition tracking loop (DTTL).

Specifically, the in-phase channel accumulates over a symbol followed by a hard decision on the signal polarity. By subtracting two successive decisions, a transition detector is used to determine whether a no transition (0), a $+1$ to -1 transition, or a -1 to $+1$ transition occurred. The quadrature channel, on the other hand, accumulates over the estimated symbol transition and, after an appropriate delay, is multiplied by the in-phase channel output, I_k. The multiplication results in an error signal, e_k, that is proportional to the estimate of the phase (or timing) error. Subsequently, e_k is multiplied by[1] κ and then filtered with the resulting output being used to control the timing generator.

The performance of the DTTL, assuming equally likely transmitted symbols, was first reported on in [4–6]. Later, the loop performance for an arbitrary transition density, assuming that the noise spectrum of the error signal is independent of the transition density, was derived in [7]. More recently, the change in noise spectrum, as well as other effects,[2] assuming a high symbol SNR and a DTTL window of one, was accounted for in [8,9]. The results, nevertheless, were used as approximations for lower symbol SNRs. The steady-state timing jitter given in [9] was simulated in [10], and it was shown therein that, at a high symbol SNR, theory and simulation agree very well, while, at a low symbol SNR (4 dB or less), theory is more optimistic than simulation. In this article, we extend the results of [9] and show the performance of the DTTL, taking into account data transition variation for all symbol SNRs and window sizes of interest. We are interested in the low symbol SNR region primarily due to the expected use of higher rate codes (1/4 and 1/6) in future space missions, which, consequently, result in lower symbol SNRs.

In the following sections, we determine the performance of the DTTL as a function of data transition variation. In particular, Section II illustrates the DTTL model, which is used in Section III to derive the timing jitter. Afterwards, in Section IV, we assess the impact of data transition variation on the probability of acquisition, and conclude with the main points of the article in Section V.

II. The DTTL Model

Consider the DTTL shown in Fig. 1 with a nonreturn-to-zero (NRZ) signaling format. Assuming that the carrier and subcarrier (if any) have been removed in an ideal fashion, the received baseband waveform is given by

[1] The factor κ (which is defined later) is used to normalize the error signal so that it is only proportional to the phase difference between the transmitted and received symbol timing.

[2] Data asymmetry, the unequal rise and fall times of the logic gating circuits, also results in additional system loss, but is not considered here.

$$r(t) = \sqrt{S}\sum_{k} d_k p(t - kT - \epsilon) + n(t) \tag{1}$$

where S is the data power, T is the symbol time, $n(t)$ is white Gaussian noise with one-sided power spectral density N_0 W/Hz, ϵ is the random epoch to be estimated, $p(t)$ is the square-wave function having a value of 1 for $0 \leq t < T$ and having value 0 elsewhere,[3] and d_k represents the kth symbol polarity with p and q representing the a priori probabilities of the data d_k taking on values 1 and -1, respectively. The data transition density for a purely random sequence can now be defined as $p_t = 2pq$, which is the measure of the data pattern variation and ranges from zero to 0.5. Let the phase error λ (in cycles) be defined as

$$\lambda = \frac{\epsilon - \widehat{\epsilon}}{T} \tag{2}$$

where ϵ is the received symbol phase and $\widehat{\epsilon}$ is the estimated symbol phase. It is clear that the error signal is affected by λ, and in order to quantify this effect, we define the following variables: λT is the timing error in seconds and $\xi_0 T$ is the quadrature integration window. In terms of these variables, the error signal, e_k, shown in Fig. 2 can now be written as follows:

$$\begin{aligned} e_k = \frac{1}{2}\Big\{&\sqrt{S}\left[(0.5\xi_0 + \lambda)Td_{k+1} + (0.5\xi_0 - \lambda)Td_k\right] + V_2 + N_1 + N_2\Big\} \\ &\times \operatorname{sgn}\Big[\sqrt{S}\left[(1-\lambda)Td_{k+1} + \lambda T d_{k+2}\right] + N_2 + N_3 + V_1\Big] \\ &- \operatorname{sgn}\Big[\sqrt{S}\left[(1-\lambda)Td_k + \lambda T d_{k+1}\right] + V_1 + V_2 + N_1\Big] \qquad \lambda \geq 0 \end{aligned} \tag{3}$$

where sgn[·] denotes the signum function; V_1 and V_2 are the noise components in the kth symbol; N_1, N_2, and N_3 are the noise components in the $(k+1)$th symbol; and W_1 is the noise component in the $(k+2)$th symbol as shown in Fig. 2, and they are all independent of each other.

III. DTTL Tracking Performance

One of the key performance measures of the DTTL is the steady-state timing jitter of λ, namely, σ_λ^2. Using linear theory, σ_λ^2 can be derived once the following two quantities are determined: (1) the loop S-curve $g(\lambda)$ as a function of the normalized timing λ and (2) the two-sided spectral density $S(\omega, \lambda)$ of the equivalent additive noise $n_\lambda(t)$.

The normalized S-curve $g_n(\lambda)$ is defined as follows:

$$g_n(\lambda, p_t) = \frac{g(\lambda)}{g'(0)|_{R_s \to \infty, p_t = 0.5}} = \frac{E_{n,s}[e_k|\lambda]}{\sqrt{S}T} \tag{4}$$

where $E_{n,s}[\cdot]$ represents expectation over the signal and noise and $R_s = ST/N_0$ is the symbol SNR. The exact closed-form solution of $g_n(\lambda, p_t)$ can be shown to be

[3] We assume the DTTL is operating in a wideband channel so that the received pulses are perfectly square, i.e., no intersymbol interference.

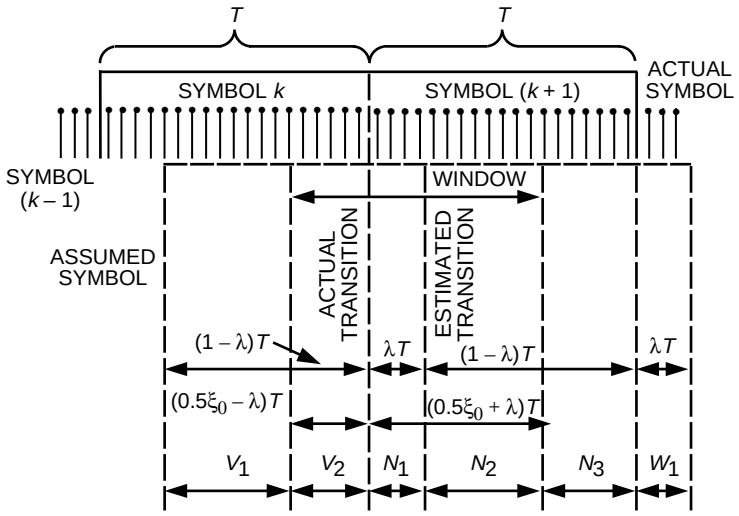

Fig. 2. The DTTL model.

$$g_n(\lambda, p_t) = \frac{1}{4}p_t(\xi_0 + 6\lambda)\left[\text{erf}\left(\sqrt{R_s}(1-2\lambda)\right)\right] - \frac{1}{4}p_t(\xi_0 - 2\lambda)\left[\text{erf}\left(\sqrt{R_s}\right)\right] \quad \text{for} \quad |\lambda| \leq \frac{\xi_0}{2} \tag{5}$$

where the error function is defined as $\text{erf}(x) = 2/\left(\sqrt{\pi}\right)\int_0^x \exp(-v^2)dv$. Figure 3 shows the normalized S-curve as a function of transition density at a low (−5 dB) symbol SNR, and it is evident that the average error becomes small as the transition density decreases. This effect is due to most of the I_k values in Fig. 1, as well as the additional noise in the error signal, being zero. The first derivative of the S-curve at λ=0, termed the slope of the S-curve, can be shown to be

$$g_n'(0, p_t) = 2p_t\text{erf}\left(\sqrt{R_s}\right) - p_t\xi_0\sqrt{\frac{R_s}{\pi}}\exp\left(-R_s\right) \tag{6}$$

which is identical to the slope given in [9] at high[4] R_s. Figure 4 shows the slope as a function of symbol SNR and transition density for a DTTL window of 0.25. It is evident that at high R_s the slope approaches $2p_t$, but this value drops as R_s decreases.

Assuming that $B_LT << 1$, it is sufficient to approximate $S(\omega, \lambda)$, the spectrum of the additive noise $n_\lambda(t)$, at zero frequency; that is, $S(0, \lambda)$. The normalized noise spectrum can be defined as

$$h(\lambda) = \frac{S(0,\lambda)}{S(0,0)|_{R_s\to\infty, p_t=0.5}} = \frac{S(0,\lambda)}{(1/4)\xi_0 N_0 T} \tag{7}$$

where $S(0, \lambda) = R(0, \lambda) + 2R(1, \lambda)$; $R(0, \lambda) = E_{n,s}[e_k e_k]$; and $R(1, \lambda) = E_{n,s}[e_k e_{k+1}]$. In addition, we consider the DTTL only at a loop SNR[5] greater than 10 dB, so $h(\lambda)$ is essentially the noise spectral density seen by the loop at λ=0; that is, $h(0)$. It can be shown that

[4] Observe that $\text{erf}\left(\sqrt{R_s}\right) \simeq 1$ and $\exp\left(-R_s\right) \simeq 0$ at a symbol SNR greater than 8 dB.

[5] Experience has shown that when the loop SNR, $\rho = 1/4\pi^2\sigma_\lambda^2$, is below 10 dB, the loop experiences cycle slipping.

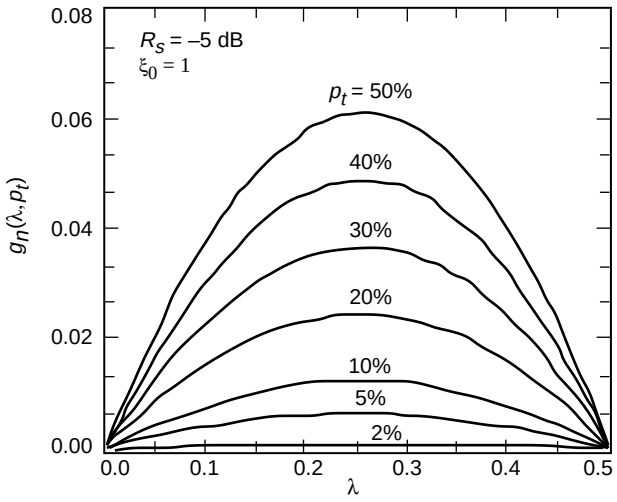

Fig. 3. Normalized S-curve with transition density at R_S = –5 dB.

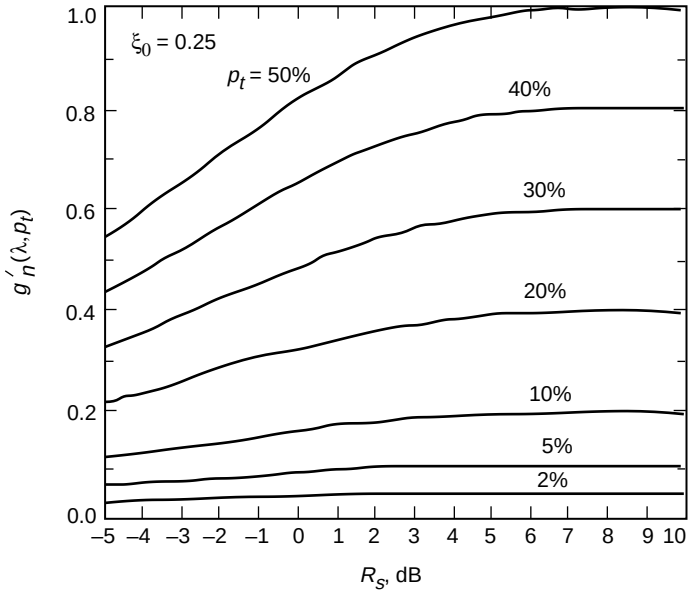

Fig. 4. Normalized slope with transition density at ξ_0 = 0.25.

$h(0) =$

$$1 + p_t\xi_0 R_s - \frac{1}{2}\left[(2p_t\left(R_s\xi_0 - 2\right) + 2)\left[\mathrm{erf}\left(\sqrt{R_s}\right)\right]^2 + 4p_t\sqrt{\frac{R_s}{\pi}}\exp\left(-R_s\right)\mathrm{erf}\left(\sqrt{R_s}\right) + \frac{\xi_0}{\pi}\left[\exp\left(-R_s\right)\right]^2\right] \tag{8}$$

which is identical to $h(0)$ given in [9] at high symbol SNR and ξ_0=1. Figure 5 shows the normalized noise spectrum as a function of symbol SNR with transition density as a parameter for $\xi_0 = 0.25$. As shown therein, at high symbol SNRs, $h(0)$ behaves as $2p_t$, while at low symbol SNRs, $h(0)$ can deviate considerably from $2p_t$.

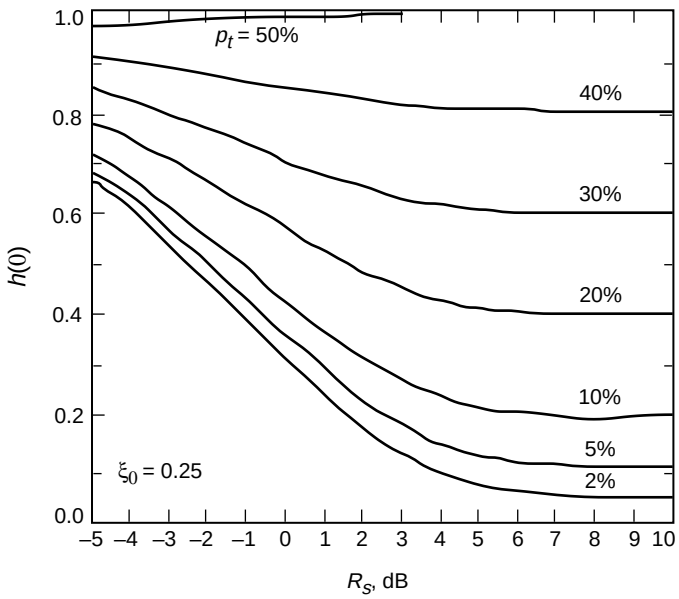

Fig. 5. Normalized noise spectrum at $\xi_0 = 0.25$.

Assuming linear theory, $g_n(\lambda, p_t)$ can be approximated as $g_n^{'}(0, p_t)\lambda$, and the variance of λ becomes [1]

$$\sigma_\lambda^2 = \frac{h(0) B_L T \xi_0}{2R_s[g_n'(0,p_t)]^2}\Phi(c) \tag{9}$$

where $\Phi(c) = B_L^*(c)/B_L$, B_L is the design loop bandwidth, and $B_L^*(c)$ is the actual noise-equivalent loop bandwidth defined as [11]

$$B_L^*(\mathrm{c}) = \frac{1}{2T}\ \frac{1}{H^2(1)}\ \frac{1}{2\pi j}\oint_{|z|=1} H(z)H\left(z^{-1}\right)\frac{dz}{z} \tag{10}$$

where[6] c is a constant that multiplies λ at the input of the loop filter (i.e., cλ). The closed-loop transfer function $H(z)$ in Eq. (10) is given as

$$H(z) = \frac{\mathrm{c}F(z)N(z)}{1 + cF(z)N(z)} \tag{11}$$

where $N(z) = T/[z^2(z-1)]$ is the numerically controlled oscillator (NCO) transfer function and $F(z)$ is the loop filter transfer function. A first-order loop filter has a form (Type I)

$$F(z) = 4B_L \tag{12}$$

and a second-order loop filter has a form (Type II)

$$F(z) = G_1 + \frac{G_2}{(1 - z^{-1})} \tag{13}$$

[6] The above two-sided complex integral can be evaluated using techniques described in [12].

where $G_1 = rd/T$, $G_2 = rd^2/T$, and $d = 4B_LT/(r-1)$, with the parameter r typically having value 2 or 4. For small B_LT products, it can be shown that, for Type I loop filters, $\Phi(c) = c$, while for Type II loop filters, $\Phi(c) > c$. In this article, we present the tracking performance of the DTTL only for a Type I loop filter.

For the DTTL, the S-curve should be normalized by $g_n^{'}(0, p_t)$, so that the loop makes adjustments only to λ. In practice, however, the knowledge of p_t is not available, and we must instead normalize the S-curve by $g_n^{'}(0, 0.5)$, so that the normalization factor in Fig. 1 becomes $\kappa = 1/[g_n^{'}(0, 0.5)]$. Consequently, the input to the loop filter is $[g_n^{'}(0, p_t)]/[g_n^{'}(0, 0.5)]\lambda = 2p_t\lambda$, so that c $= 2p_t$. For a Type I loop filter, the timing jitter can be rewritten by absorbing the factor $[g_n^{'}(0, p_t)]/[g_n^{'}(0, 0.5)]$ into the bandwidth, B_L. Disregarding $\Phi(0)$, the variance consequently becomes

$$\sigma_\lambda^2 = \frac{h(0)B_{L0}T\xi_0}{2R_s g_n^{'}(0, p_t) g_n^{'}(0, 0.5)} \tag{14}$$

where B_{L0} is the single-sided bandwidth at $p_t = 0.5$. Note that the above variance is identical to that given in [9] at high symbol SNRs, since $g_n^{'}(0, 0.5) = 1$ in that region. The ratio of the variance given in Eq. (9) to that given in [9] is plotted as a function of symbol SNR in Fig. 6(a). It is clear that, at high symbol SNRs, the two results match as expected while, at lower symbol SNRs, they diverge by as much as 5 dB. Figure 6(b), on the other hand, shows the variance as a function of symbol SNR for window sizes 1 and 0.25. It is evident that, at high symbol SNRs, the variance is independent of p_t while, at low symbol SNRs, the variance increases for decreasing p_t. The horizontal line in Fig. 6(b) represents the 10-dB loop SNR threshold, and operating above this line can cause cycle slipping. Simulation was conducted to verify the analysis as shown in Fig. 6(b) for a $B_{L0}T$ product of 0.01. Below the 10-dB loop SNR line, simulation and theory agree very well, while above it, linear theory breaks down and theory is more optimistic than simulation.

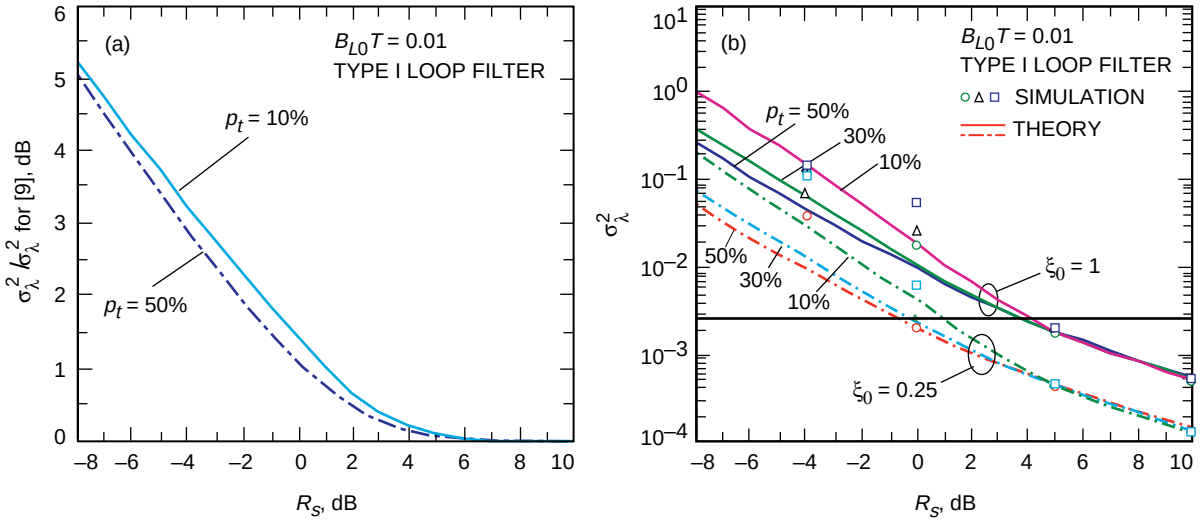

Fig. 6. Steady-state timing jitter performance: (a) the ratio of σ_λ^2 given in Eq. (9) to σ_λ^2 given in [9] versus symbol SNR and (b) symbol timing jitter versus symbol SNR for a Type I loop filter using ξ_0 = 1 and 0.25.

IV. DTTL Acquisition Performance

Now that the tracking performance of the DTTL for varying data transition densities is characterized, we investigate its acquisition performance in this environment. Unfortunately, there is no easy analytical way to study the acquisition performance of the DTTL, and we resort to simulation to understand its behavior. Throughout the simulation, a sampling rate of 100 Hz and a symbol rate of 1 Hz are maintained so that there are 100 samples per symbol in each symbol duration. Each simulation was run for $100/B_L$ seconds and, if the difference between the NCO phase and the input phase is within the absolute value of $\pi/2$ for $10/B_L$ seconds (our lock criterion), the simulation stops and records the normalized time. The simulation was run 200 times for different noise seeds (i.e., different input phases) in order to produce sufficient statistics for the cumulative probability distribution. In the simulation, a Type II loop filter with $r = 2$ was used with $B_L = 0.0001$ Hz and the same NCO transfer function as in the tracking case.

As shown in Fig. 7, numerous simulations were run to understand the behavior of the DTTL in the presence of p_t. In particular, Fig. 7(a) shows the probability of acquisition for $\Delta f/B_L = 0$ and 0.25 at a symbol SNR of 0 dB. Without any frequency offset, the $B_L t$ (normalized acquisition) time for an acquisition probability (P_{acq}) of 90 percent is 0.6, 0.8, and 10.0 for p_t =50, 30, and 10 percent, respectively. With a frequency offset equal to $0.25B_L$, on the other hand, the $B_L t$ time for $P_{acq} = 90$ percent is 0.6, 2.0, and 20.0 for p_t =50, 30, and 10 percent, respectively. It is clear that a frequency offset of $0.25B_L$ has little effect on the acquisition time for $p_t = 0.5$. In addition, Fig. 7(b) shows the probability of acquisition for $\Delta f/B_L = 0.75$ again at a 0-dB symbol SNR. We have added the case of $\Delta f/B_L = 0$ therein as a reference for comparison. For the $\Delta f/B_L = 0.75$ case, the $B_L t$ time for $P_{acq} = 90$ percent is 3.0 and 10.0 for $p_t = 50$ and 30 percent, respectively, while the case for $p_t = 10$ percent never locks within $100/B_L$ seconds. In general, the acquisition time for $p_t = 50$ percent is a magnitude lower than $p_t = 10$ percent, but only slightly less for $p_t = 30$ percent.

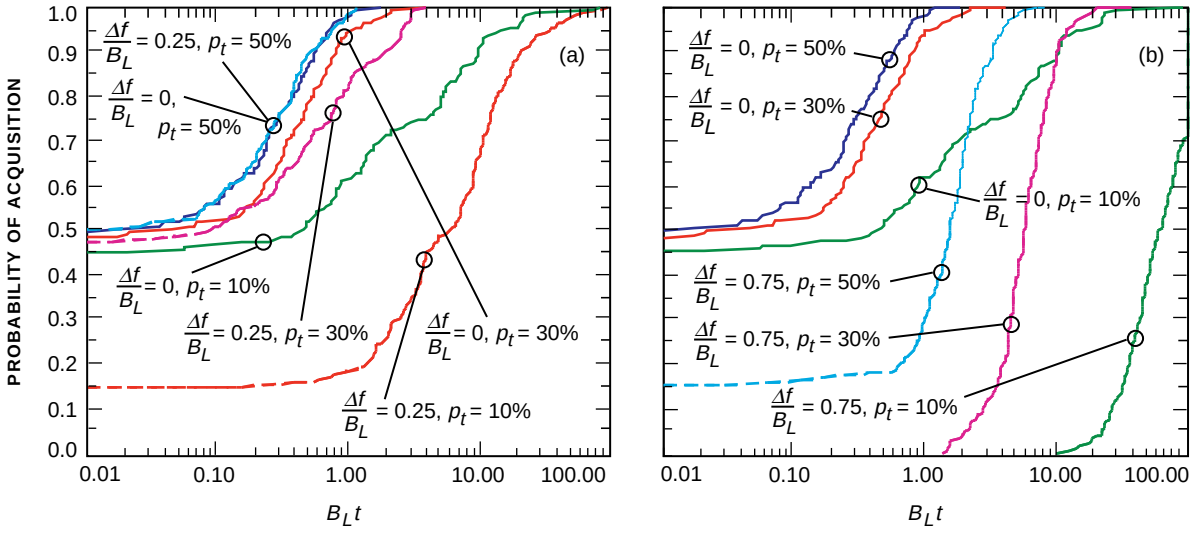

Fig. 7. The probability of acquisition versus normalized time at R_s = 0 dB at (a) $\Delta f/B_L$ = 0 and 0.25 and (b) = $\Delta f/B_L$ = 0.75.

V. Conclusion

This article presented the tracking and acquisition performance of the DTTL symbol synchronizer under various conditions of transition density and window size. For a Type I loop filter, the tracking performance at high symbol SNRs is independent of the transition density, but at low symbol SNRs, severe degradation can result for low transition density. The acquisition performance of the DTTL was simulated at a 0-dB symbol SNR. As a rough rule, the acquisition time for $p_t = 10$ percent is ten times longer than that for $p_t = 50$ percent.

References

[1] W. C. Lindsey and M. K. Simon, *Telecommunication Systems Engineering*, Englewood Cliffs, New Jersey: Prentice-Hall Inc., 1973.

[2] S. Hinedi, "NASA's Next Generation All-Digital Deep Space Network Breadboard Receiver," *IEEE Trans. on Commun.*, vol. 41, pp. 246–257, January 1993.

[3] *Tracking and Data Relay Satellite System (TDRSS) Users' Guide*, Revision 5, STDN 101.2, Goddard Space Flight Center, Greenbelt, Maryland, September 1984.

[4] W. C. Lindsey and R. C. Tausworthe, "Digital Data-Transition Tracking Loops," *Space Programs Summary 37-50*, Jet Propulsion Laboratory, Pasadena, California, vol. III, pp. 272–276, April 1968.

[5] M. K. Simon, "Analysis of the Steady State Phase Noise Performance of a Digital Data-Transition Tracking Loop," *Space Programs Summary 37-55*, Jet Propulsion Laboratory, Pasadena, California, vol. 3, pp. 54–62, February 1969.

[6] W. J. Hurd and T. O. Anderson, "Digital Transition Tracking Symbol Synchronizer for Low SNR Coded Systems," *IEEE Trans. on Commun. Technology*, vol. COM-18, pp. 589–596, October 1970.

[7] T. M. Nguyen and S. Hinedi, "Effects of the Transition Density on the Performance of Data-Derived Symbol Synchronizer," *Proceedings of ESA/ESTEC*, Session 4, Noordjwik, The Netherlands, pp. 35–51, September 1992.

[8] C. S. Tsang and W. C. Lindsey, "Bit Synchronization in the Presence of Asymmetric Channel Noise," *IEEE Trans. on Commun.*, vol. COM-34, pp. 528–537, June 1986.

[9] C. S. Tsang and C. M. Chie, "Effect of Signal Transition Variation on Bit Synchronizer Performance," *IEEE Trans. on Commun.*, vol. 41, no. 5, pp. 673–677, May 1993.

[10] S. Hinedi, T. M. Nguyen, and A. Anabtawi, "Minimum Symbol Transition Density on Earth-to-Space Links," *Consultative Committee for Space Data Systems, Report of the Proceedings of the RF and Modulation Subpanel 1E Meeting*, Consultative Committee for Space Data Systems German Space Operation Center, September 20–24, 1993, CCSDS B20.0-Y-1, Yellow Book, February 1994.

[11] S. Aguirre and W. J. Hurd, "Design and Performance of Sampled Data Loops for Subcarrier and Carrier Tracking," *The Telecommunications and Data Acquisition Progress Report 42-79, July–September 1984*, Jet Propulsion Laboratory, Pasadena, California, pp. 81–95, November 15, 1984.

[12] R. Winkelstein, "Closed Form Evaluation of Symmetric Two-Sided Complex Integrals," *The Telecommunications and Data Acquisition Progress Report 42-65, July–August 1981*, Jet Propulsion Laboratory, Pasadena, California, pp. 133–141, October 15, 1981.